



HAL
open science

Characterization and modeling of 2DEG mobility in AlGaN/AlN/GaN MIS-HEMT

I. Nifa, C. Leroux, A. Torrès, M. Charles, G. Reimbold, G. Ghibaudo, E. Bano

► **To cite this version:**

I. Nifa, C. Leroux, A. Torrès, M. Charles, G. Reimbold, et al.. Characterization and modeling of 2DEG mobility in AlGaN/AlN/GaN MIS-HEMT. *Microelectronic Engineering*, 2019, 215, pp.110976. 10.1016/j.mee.2019.05.003 . hal-02145457

HAL Id: hal-02145457

<https://hal.science/hal-02145457>

Submitted on 25 Oct 2021

HAL is a multi-disciplinary open access archive for the deposit and dissemination of scientific research documents, whether they are published or not. The documents may come from teaching and research institutions in France or abroad, or from public or private research centers.

L'archive ouverte pluridisciplinaire **HAL**, est destinée au dépôt et à la diffusion de documents scientifiques de niveau recherche, publiés ou non, émanant des établissements d'enseignement et de recherche français ou étrangers, des laboratoires publics ou privés.



Distributed under a Creative Commons Attribution - NonCommercial 4.0 International License

Characterization and modelling of 2DEG mobility in AlGa_{0.25}N/AIn/GaN MIS-HEMT

I. Nifa, C. Leroux, A. Torres, M. Charles, G. Reimbold, G. Ghibaudo and E. Bano

Abstract—We present a detailed study of the process influence on two-dimensional electron gas (2DEG) transport properties in Al_{0.25}Ga_{0.75}N/AIn/GaN heterostructure. Hall effect measurements are used to analyze the conduction in normally on devices demonstrating the formation of a second channel at the Al₂O₃/AlGa_{0.25}N interface for high biases. Electrical characterization is performed on a large set of devices for temperatures ranging from 25°C to 250°C, and 2DEG mobility is extracted using split C-V measurement technique. Various technological splits were experimentally tested and the corresponding mobility characteristics were modeled using the Kubo-Greenwood formula in order to determine the dominant scattering phenomenon limiting the 2DEG mobility.

Keywords—GaN-HEMT; 2DEG mobility; Hall effect, Coulomb scattering; Optical phonons scattering; Normally-On; Normally-Off

This research was supported by ENIAC and The National Centre for Research and Development (Grants ENIAC-2012- 2/1/2013 and ENIAC-2012-2/2/2013) through project AGATE (‘Development of Advanced GaN substrates & Technologies’)

Iliass Nifa, Charles Leroux, Alphonse Torres, Matthew Charles and Gilles Reimbold are with Univ. Grenoble Alpes. CEA-LETI, MINATEC, Grenoble, France (e-mail: charles.leroux@cea.fr)

G rard Ghibaudo and Edwige Bano are with Univ. Grenoble Alpes. IMEP-LAHC, MINATEC/INPG, Grenoble France

I. INTRODUCTION

AlGa_{0.25}N/GaN high electron mobility transistors (HEMTs) on Si substrates are one of the best candidates for power and RF applications, with operating temperature for power applications ranging between 150°C and 250°C [1]. The HEMT on-state resistance is a critical issue. Understanding the influence of process steps on the two-dimensional electron gas (2DEG) properties is a key step for further improvement of GaN-HEMT devices. This study focuses on the impact of the gate fabrication process on the electron conduction of AlGa_{0.25}N/GaN MIS-HEMTs. Through detailed characterization and dedicated modelling, we carefully analyze the location of electron conduction and the origin of scattering phenomena limiting their mobility.

II. EXPERIMENTAL

II.1 Device Fabrication

An Al_{0.25}Ga_{0.75}N/AIn/GaN heterostructure (Fig.1) is grown by Metal-Organic Chemical Vapor Deposition (MOCVD), on a 200 mm diameter silicon (111) substrate. An AlN nucleation layer is first deposited on the silicon followed by AlGa_{0.25}N transition layer and GaN (≥1μm of thickness) buffer layers. An AlN spacer of a fixed thickness

of 1 nm and an Al_{0.25}Ga_{0.75}N barrier layer are then grown on top of the previous stack, followed by ex-situ deposition of a Si₃N₄ passivation layer which is etched according to three different etching processes: Inductive Coupled Plasma technique (ICP), Reactive Ion etching and ICP followed by 10nm chlorine-based over etching.

The etching was followed by the deposition of an oxide layer of Al₂O₃ by Atomic layer deposition (ALD) and a TiN(60nm)/W(300nm) metallic gate. The Source and Drain are composed of metallic ohmic contacts (Ti/AlCu) connected to the 2DEG. Eight different samples have been characterized. Table 1 summarizes the most important stack parameters of these samples designed for the study of the impact of 3 main parameters i.e. AlGa_{0.25}N barrier layer thickness, gate etching process and HEMT technology (normally on&off).

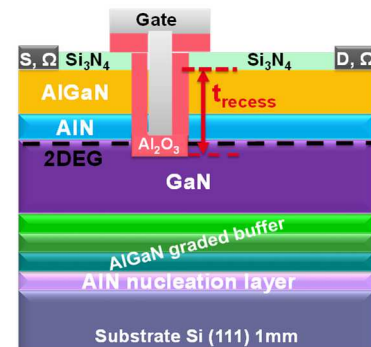


Fig. 1. : A schematic of an Al_{0.25}Ga_{0.75}N/AIn/GaN MIS-HEMT stack.

Split name	Wafer name	Al ₂ O ₃ thickness (nm)	AlGa _{0.25} N thickness (nm)	AlN thickness (nm)	GaN thickness (μm)	Si ₃ N ₄ etching	type of HEMT
AlGa _{0.25} N barrier layer thickness	A	20	24	1	1	ICP	Normally-On
	B	20	17	1	1	ICP	Normally-On
	C	20	10	1	1	ICP	Normally-On
	D	6	24	1	1	ICP	Normally-On
etching process used to etch Si ₃ N ₄ passivation layer	E	6	24	1	1	RIE	Normally-On
	F	6	24	1	1	ICP+10nm Cl-based over etching	Normally-On
Normally-On VS Normally-Off technology	G	30	14 (partial recess of 10 nm from AlGa _{0.25} N barrier)	1	2	ICP	Normally-On
	H	30	0 (full recess+10nm etched from GaN layer)	1	2	ICP	Normally-Off

TABLE I. DESCRIPTION OF STUDIED SPLITS.

AlGaIn barrier layer thickness has been varied by using different epitaxy processes from 10 to 24 nm (wafer A, B and C). ICP and RIE have been compared to ICP etching technique that is followed by 10nm chlorine-based over etching (wafer D, E and F) leading each one to a certain recess of the AlGaIn layer. Wafers G and H (full recess of AlGaIn layer) are measured to compare 2DEG transport properties corresponding to normally-On versus normally-Off devices. Moreover, these devices are compared to a gate-less device corresponding to the access region and for which no gate fabrication process related degradation is expected.

II.2 Experimental methodology

Effective mobility measurements have been performed on a “gated” Hall bar [2] (Fig.2) allowing both measurements of the sheet channel resistance R_{2DEG} and the electron concentration N_{2DEG} . The 2DEG effective mobility μ_{2DEG} is then extracted for each temperature ranging from 25 to 250°C using Eq.1.

$$\mu_{2DEG}(V_g, T) = \frac{1}{q \cdot R_{2DEG}(V_g, T) \cdot N_{2DEG}(V_g, T)} \quad (1)$$

Where q is the elementary electron charge, T is the temperature, V_g is the gate voltage. R_{2DEG} and N_{2DEG} parameters are obtained from I-V and C-V characteristics, respectively.

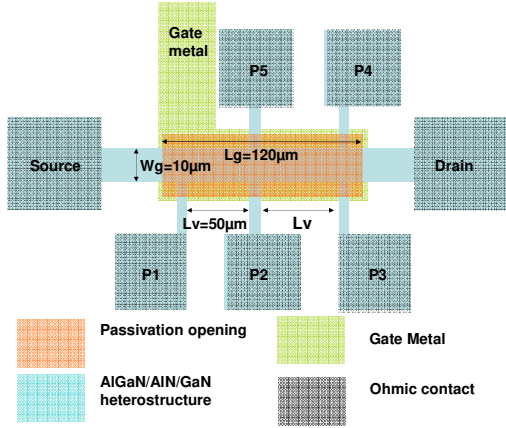


Fig. 2. : Layout of the “gated” Hall bar structure ($L_g = 120 \mu m$; $W_g = 10 \mu m$) used to characterize μ_{2DEG} electron mobility.

Precise measurements of $R_{2DEG}(V_g)$ are obtained using the additional ohmic contacts P_i ($i=1,2,..5$) connected to the 2DEG as depicted in Fig. 2. R_{2DEG} is calculated by the following equation :

$$R_{2DEG}(V_g) = \frac{W_g |V_{P1}(V_g) - V_{P2}(V_g)|}{L_v I_d(V_g)} \quad (2)$$

Where W_g is the gate width, I_d the source-drain current, V_{P1} and V_{P2} the measured voltages of ohmic contacts $P1$ and $P2$ with respect to the grounded source contact. The separation distance between the contacts is given by L_v as reported in Fig. 2.

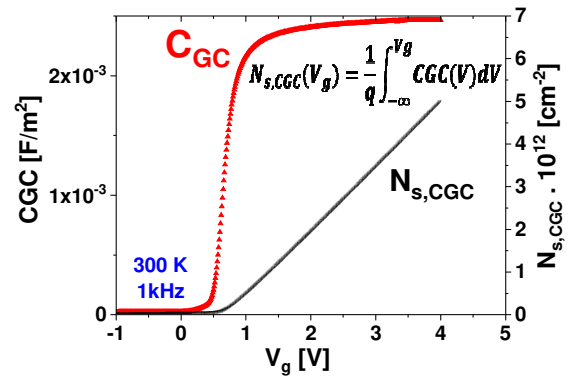


Fig. 3. Experimental $C_{GC}(V_g)$ and its corresponding $N_{s,CGC}(V_g)$ obtained on wafer H.

On the other hand, $N_{2DEG}(V_g)$ can be obtained either from gate-to-channel capacitance $C_{GC}(V_g)$ measurement or from Hall measurement. Using first capacitance measurements, $N_{2DEG}(V_g)$ is calculated by the integration of $C_{GC}(V_g)$ curves as shown in Fig. 3. $N_{2DEG}(V_g)$ is given by:

$$N_{2DEG}(V_g) = \frac{1}{q} \int_{-\infty}^{V_g} C_{GC}(V) dV \quad (3)$$

Most results presented hereafter have been obtained through this split CV methodology [3], nevertheless in order to investigate specific transport properties of the 2DEG at large $V_g - V_t$ overdrive, CV and Hall effect measurements have been performed and compared on the same gated Hall bar (wafer D). To achieve a high precision Hall effect measurement, we have developed a new experimental set-up [4]. The resulting $N_{s,CGC}(V_g)$, $N_{s,Hall}(V_g)$, $\mu_{s,CGC}(V_g)$ and $\mu_{s,Hall}(V_g)$ characteristics are compared in Fig. 4.

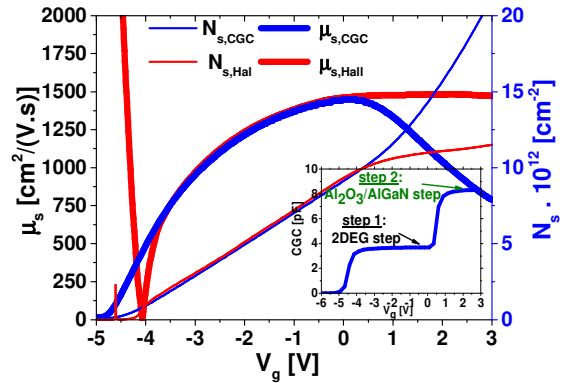


Fig. 4. Comparison between $\mu_s(V_g)$ and $N_s(V_g)$ experimental characteristics obtained by C-V and Hall effect measurements (wafer D)..

From $V_g = -4$ to $0V$, both characterization techniques give the same 2DEG mobility and concentration variation with V_g , but discrepancies are observed for the stronger accumulation regime ($V_g > 0$), when the capacitance increases towards a second plateau (see insert of Fig. 4). This behavior can be explained by the formation of an accumulation layer at the AlGaIn/Al₂O₃ interface (named channel 2 hereafter) [5], in addition to the classical 2DEG at the AlGaIn/GaN interface (channel 1 hereafter). $N_{s,CGC}(V_g)$ obtained through the integration of $C_{GC}(V_g)$ will give the sum of the concentrations in both channels, whereas Hall Effect measurement lead to a much more complex analysis (Eq. 4), for which the carrier density of the channel with the largest mobility prevails [6]:

$$N_{s,Hall} = \frac{(N_{s,1}\mu_{s,1} + N_{s,2}\mu_{s,2})^2}{N_{s,1}\mu_{s,1}^2 + N_{s,2}\mu_{s,2}^2} \quad (4)$$

Considering that the measured HEMT sheet resistance corresponds to the two channel resistances in parallel, the two different estimations of the electron concentration will lead through Eq. 1 to two different estimations of electron mobility $\mu_{s,Hall}(V_g)$ and $\mu_{s,CGC}(V_g)$ (Eq.5&6):

$$\mu_{s,Hall} = \frac{N_{s,1}\mu_{s,1}^2 + N_{s,2}\mu_{s,2}^2}{N_{s,1}\mu_{s,1} + N_{s,2}\mu_{s,2}} \quad (5)$$

$$\mu_{s,CGC} = \frac{N_{s,1}\mu_{s,1} + N_{s,2}\mu_{s,2}}{N_{s,1} + N_{s,2}} \quad (6)$$

Observed differences on the estimations of 2DEG mobility and concentration (Fig.4) can then be better understood. $N_{s,CGC}$ estimates not only the 2DEG concentration, but also takes into account of the formation of the second channel having probably a lower electron mobility, and leads thus to a “false” 2DEG effective mobility (Fig. 4). In fact, $\mu_{s,CGC}$ is an average mobility of all free electrons, and is not representative of the sole 2DEG conduction. On the contrary, for $V_g > 0V$, $N_{s,Hall}$ remains constant being more representative of the 2DEG concentration that no longer increases with V_g , being screened by the upper channel. Thus, its associated mobility remains logically constant. To validate such an hypothesis, we have self-consistently solved Eqs 3, 4, 5 and 6 assuming that $\mu_{s,2} \ll \mu_{s,1}$. In Fig. 5, we show the extracted carrier mobility versus its concentration for 2DEG (channel 1) and electron accumulation at AlGa_N/Al₂O₃ interface (channel 2) compared to experimental characteristics ($N_{s,CGC}$, $N_{s,Hall}$, $\mu_{s,CGC}$ and $\mu_{s,Hall}$). We can notice in Fig.5: first, Hall measurement gives the better estimation of electron mobility in such devices; second, there is a large difference between the 2DEG mobility and the mobility of electron accumulated at the AlGa_N/Al₂O₃ interface.

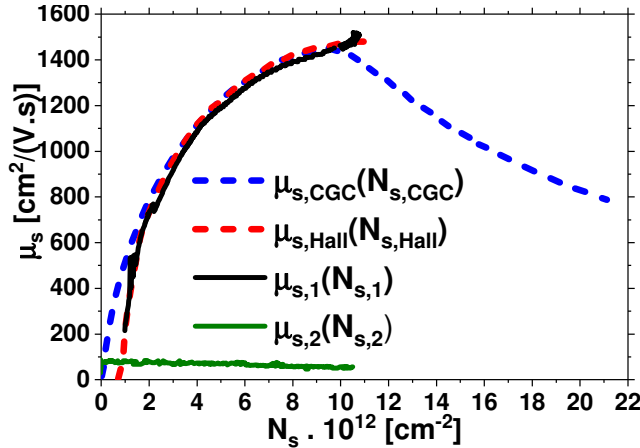


Fig. 5. $\mu_s(N_g)$ characteristics (in solid line) obtained by C-V and Hall effect measurements (wafer D) compared to $\mu_{s,1}(N_{g,1})$ and $\mu_{s,2}(N_{g,2})$ obtained using self-consistent extraction from previous data (Fig. 4).

III. RESULTS AND DISCUSSION

III.1 Experimental results

The dependence of electron mobility with temperature has been measured on the various splits described in Table 1. Mobility values have been extracted using CGC and R_{2DEG} , but for all measurements, V_g biases have been kept below the onset of the upper channel at the AlGa_N/Al₂O₃ interface. In Fig. 6, the $\mu_{2DEG}(N_{2DEG})$ are reported for Samples A, B&C from 25°C to 250°C. From $t_{AlGaN}=24nm$ to $t_{AlGaN}=17nm$, only a slight decrease in $\mu_{2DEG}(N_{2DEG},T)$ is observed, but

decrease of t_{AlGaN} to 10nm induces a serious reduction of the 2DEG mobility.

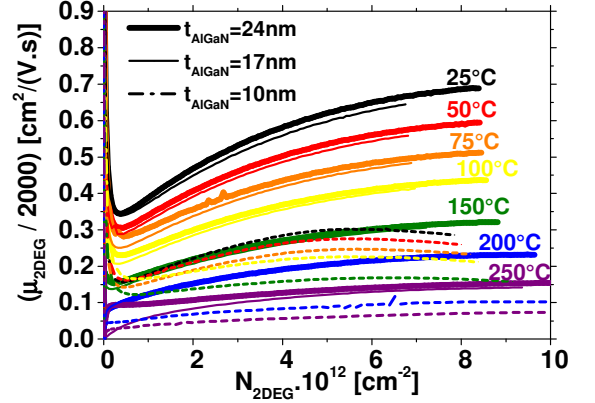


Fig. 6. $\mu_{2DEG}(N_{2DEG})$ characteristics for temperatures from 25° to 250°C for AlGa_N barrier layer thickness split.

To investigate the influence of Si₃N₄ passivation layer etching process, the same $\mu_{2DEG}(N_{2DEG})$ characteristics were extracted for samples D, E and F, for temperatures from 25° to 250°C (Fig. 7). At 25°C, a severe degradation is noticed for RIE-etching-processed sample where the 2DEG mobility drops drastically to 200 cm²/(V.s) while it reaches almost 1800 cm²/(V.s) for ICP-10nm Cl-based over etching sample (wafer F). This behavior could be explained by the expected fluorine implantation profile associated with the RIE etching process [7] [8] and will be investigated in the next section.

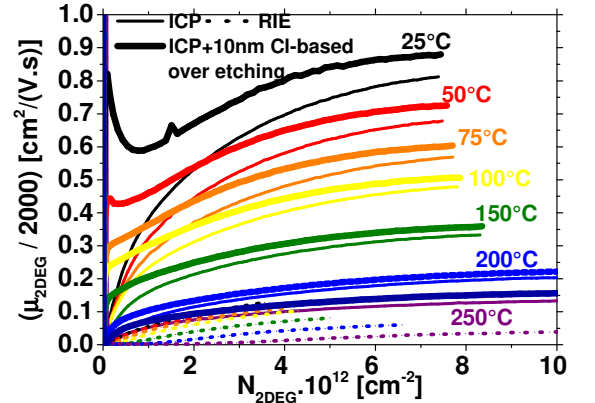


Fig. 7. $\mu_{2DEG}(N_{2DEG})$ characteristics for temperatures from 25° to 250°C for etching processes used to remove Si₃N₄ passivation layer split

The difference in 2DEG mobility between Normally-On/Off technologies is reported in Fig. 8. The shape and values observed in $\mu_{2DEG}(N_{2DEG})$ characteristics for both technologies are different. Indeed, for the Normally-Off sample, the channel is no longer naturally formed, and needs a positive V_g to enhance electron accumulation under the gate. In this case, the 2DEG mobility is the most degraded mobility among all studied samples, whereas, for wafer G, this mobility has almost a similar shape and values to the other Normally-On samples. Electron mobility for the normally off device is found in the range of mobility measured for the onset of electron accumulation at the AlGa_N/Al₂O₃ interface (Fig.5).

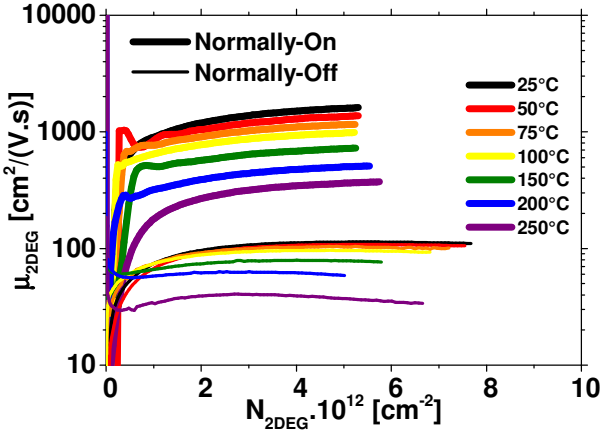


Fig. 8. $\mu_{2DEG}(N_{2DEG})$ characteristics for temperatures from 25° to 250°C for Normally-On VS Normally-Off split.

III.2 Effective mobility modelling

In order to get an better insight into the principal scattering mechanisms limiting the 2DEG mobility, single sub-band Kubo-Greenwood mobility modeling [9] adapted to AlGaIn/GaN structures [10] has been performed and compared to our set of experimental data. Table II summarizes all equations used in the Kubo-Greenwood formalism. This model takes into account acoustic and optical phonon scattering (μ_{ac} and μ_{op}) mechanisms in addition to Coulomb scattering and surface roughness scattering mechanisms (μ_C and μ_{SR}). The default parameter values used for our simulation are taken from [10] and are well representative of AlGaIn/GaN structures. However, the density of impurities N_{imp} and the surface roughness scattering μ_{SR0} parameters reported in Fig. 9 for all studied samples have been adjusted in order to match the experimental $\mu_{2DEG}(N_{2DEG})$ characteristics.

Effective mobility:

$$\mu_{eff}(N_{2DEG}, T) = \frac{\sigma(N_{2DEG}, T)}{q \cdot N_{2DEG}} \quad (7)$$

2D gas conductivity:

$$\sigma(N_{2DEG}, T) = \int_0^{+\infty} q \cdot A_{2D} \cdot E \cdot \mu_{tot}(E, N_{2DEG}, T) \left(-\frac{\partial f}{\partial E} \right) dE \quad (8)$$

Energy mobility function:

$$\frac{1}{\mu_{tot}(E, N_{2DEG}, T)} = \frac{1}{\mu_{op}(T)} + \frac{1}{\mu_{ac}(T)} + \frac{1}{\mu_C(E, N_{2DEG}, T)} + \frac{1}{\mu_{SR}(N_{2DEG})}$$

with $\mu_{op} = \mu_{op0} \cdot \left[\exp\left(\frac{\hbar\omega}{kT}\right) - 1 \right]$, $\mu_{ac} = \mu_{ac0} \cdot \frac{100}{T}$,

$$\mu_C = \mu_{C0} \cdot \frac{E}{N_{imp}} \cdot \left(\frac{\lambda + \lambda_0}{\lambda} \right)^2, \mu_{SR} = \mu_{SR0} \cdot \left(\frac{N_0}{N_s} \right)^2$$

where $\lambda(N_{2DEG}, T) = \frac{\epsilon_{sc}}{q} \cdot \frac{\partial E_F}{\partial N_{2DEG}}$ and

$$E_F(N_{2DEG}, T) = kT \cdot \ln \left[\exp\left(\frac{N_{2DEG}}{A_{2D} \cdot kT}\right) - 1 \right]$$

TABLE II. Kubo-Greenwood mobility model. Default Mobility parameters are taken from [10]. Only N_{imp} and μ_{SR0} parameters are adjusted to fit experimental data.

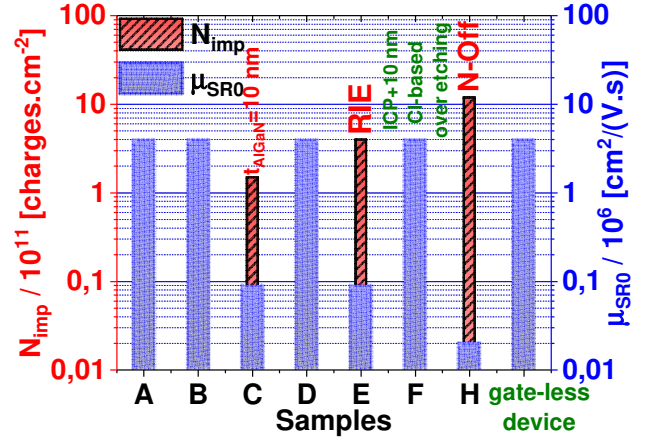


Fig. 9. N_{imp} , and μ_{SR0} , fitting parameters used in Kubo-Greenwood mobility modeling to fit for all studied samples the 2DEG mobility experimental curves.

We compare in Fig. 10 experimental (a) and simulated (b) characteristics for $\mu_{2DEG}(N_{2DEG})$ on wafer D. A very good agreement is obtained for temperatures up to 150°C. For higher temperatures, our model is less accurate for describing the 2DEG mobility variation with temperature. We suspect the onset of a parallel transport phenomenon that is occurring at the $Al_2O_3/AlGaIn$ interface, which could start even at $V_G < 0$ when the temperature is increased as was observed in $In_{0.75}Ga_{0.25}As$ MOSHEMT [6].

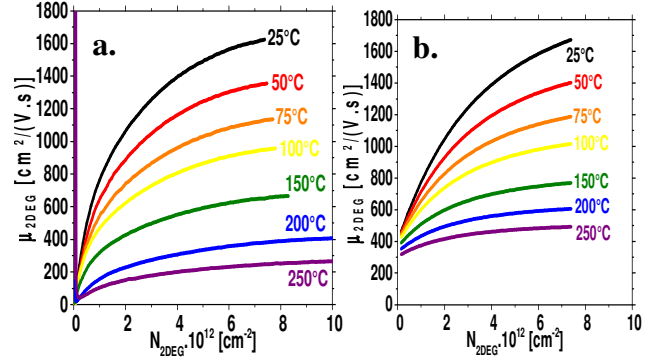


Fig. 10. $\mu_{2DEG}(N_{2DEG})$ characteristics for temperatures from 25° to 250°C performed on wafer D. a: experimental results, b: simulation with Kubo-Greenwood mobility modeling adapted to GaN material.

In Fig. 11, experimental and simulated $\mu_{2DEG}(T)$ characteristics performed on all samples are displayed for a given $N_{2DEG} = 3 \cdot 10^{12} \text{ cm}^{-2}$. The simulated curves have been obtained using the default phonon scattering parameters [10] with only N_{imp} and μ_{SR0} as fitting parameters to adjust the experimental $\mu_{2DEG}(N_{2DEG})$ data. In this way, a very good overall description of the mobility variations with temperature can be achieved for all the splits. At first glance, the strong attenuation of the temperature mobility dependence for various splits indicates that the defect-related scattering is significantly enhanced.

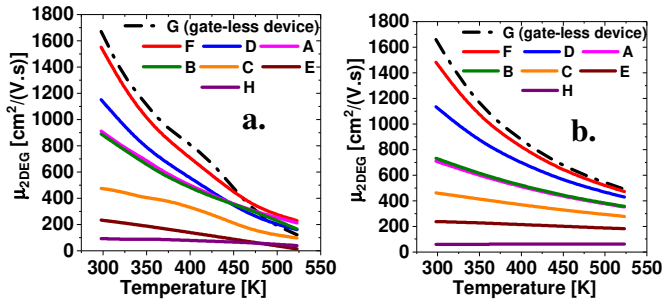


Fig. 11. $\mu_{2DEG}(T)$ characteristics for $N_{2DEG}=3.10^{12}$ cm^{-2} performed on all samples : *a*: experimentally, *b*: with Kubo-Greenwood mobility modeling adapted to GaN material. For G wafer which is similar to A wafer, $\mu_{2DEG}(T)$ has been reported for a specific device without Al_2O_3 dielectric gate.

Gate-less device has the highest 2DEG mobility confirming that gate deposition on the active layer has a negative impact on the transport properties of GaN-HEMT. The second best 2DEG mobility values are seen on the device that includes 10nm chlorine-based over etching after the ICP etching of passivation layer. On the contrary, the mobility drastically drops for devices with $t_{AlGaN}=10nm$, RIE etching process and is worse for Normally-Off technology.

Among N_{imp} and μ_{SR0} fitting parameters reported in Fig. 9, N_{imp} which accounts for the scattering and remote scattering of defects is our first order fitting parameter. A large N_{imp} is obtained with RIE etching process and it increases by one decade more in the case of a Normally-Off device. The sample with no deposited gate leads to the lowest N_{imp} and it slightly increases when a final chlorine based etching is performed for gated devices (wafer F). The surface roughness parameter is our second order fitting parameter, and it is almost the same for all samples, but we notice a degradation of surface roughness for the RIE etched (wafer E) and 10 nm AlGa_N (wafer C) and an even larger degradation for Normally-off devices (wafer H). Wafers C and E correspond to the thinnest AlGa_N layers and so this degradation could be related to a remote surface roughness increase. For normally off devices, the etched interface is in direct contact with 2DEG, and an increase of roughness would not be surprising.

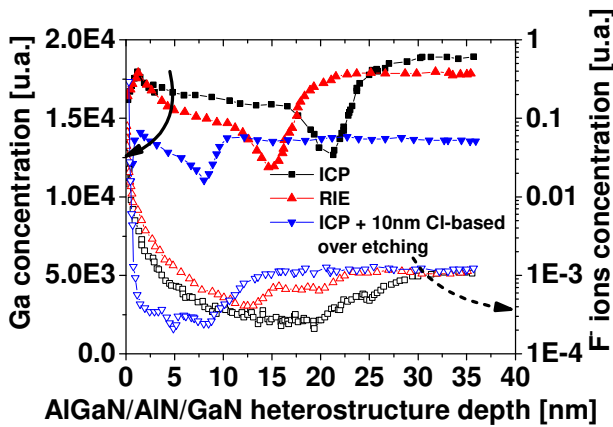


Fig. 12. SIMS characterization of $Al_{0.25}Ga_{0.75}N/AlN/GaN$ heterostructure before the gate processing. Fluorine ions concentration is presented with open symbols whereas Ga atoms concentration with solid ones.

In order to clarify why a Cl-based etching is beneficial to 2DEG mobility, a Secondary Ion Mass Spectroscopy (SIMS) characterization was performed on samples D, E and F as reported in

Fig. 12. The observed peaks in the Ga concentration profiles indicate the position of AlN/GaN interface. Fluorine ions concentration for RIE etching process is more than 2 orders of magnitude larger than for ICP+10nm Cl-based over etching process on top of the AlGa_N barrier. We conclude from this figure that chlorine-assisted etching efficiently reduces F⁻ impurities related either to ICP and even more to RIE etching process, leading to a recovery of the 2DEG mobility as shown in Fig. 11.

IV. CONCLUSION

For Normally-On devices, the comparison between Hall effect and classical split-CV measurements at higher biases has shown the formation of a conduction channel with highly degraded electron mobility at upper interface of AlGa_N layer. The 2DEG effective mobility was extracted using split-CV technique, at temperatures ranging from 25 to 250°C on $Al_{0.25}Ga_{0.75}N/AlN/GaN$ heterostructure HEMT. Experimental mobility data were analyzed using a single sub-band Kubo-Greenwood transport formalism. We observed that, for good samples, the mobility is mainly limited by phonon scattering, whereas for lower quality ones, it is mostly controlled by Coulomb scattering and surface roughness scattering mechanisms. Finally, by SIMS characterization we proved that fluorine ions introduced by ICP and RIE etching process degrade the mobility, whereas chlorine-based etching had a beneficial effect on the transport. These results prove that the high level of 2DEG mobility observed at AlGa_N/GaN heterojunction can be significantly degraded by defects induced by gate etching processes, or as we move to a GaN/dielectric interface.

REFERENCES

- [1] N. Zhang, V. Mehrotra, S. Chandrasekaran, B. Moran, L. Shen, U. Mishra, E. Etzkorn and D. Clarke, "Large area GaN HEMT power devices for power electronic applications: switching and temperature characteristics", Power Electron. Specialist Conference, vol. 1,(2003) 233–237, <https://doi.org/10.1109/PESC.2003.1218300>
- [2] A. M. Wells, M. J. Uren, R. S. Balmer, K. P. Hilton, T. Martin, and M. Missous, "Direct demonstration of the 'virtual gate' mechanism for current collapse in AlGa_N/GaN HFETs", Solid-State Electron., vol. 49, no. 2 (2005) 279–282, <https://doi.org/10.1016/j.sse.2004.10.003>
- [3] C.G. Sodini, T.W. Ekstedt, and J.L. Moll, "Charge accumulation and mobility in thin dielectric MOS transistors", Solid-State Electronics, vol. 25, n°9 (1982) 233–237, [https://doi.org/10.1016/0038-1101\(82\)90170-8](https://doi.org/10.1016/0038-1101(82)90170-8)
- [4] I. Nifa, C. Leroux, A. Torres, M. Charles, D. Blachier, G. Reimbold, G. Ghibaudo and E. Bano, "Characterization of 2DEG in AlGa_N/GaN heterostructure by Hall effect," in Microelectronic Engineering, vol. 178 (2017) 128–131, <https://doi.org/10.1016/j.mee.2017.05.009>
- [5] C. Mizue, Y.Hori, M.Miczek and T. Hashizume, "Capacitance-Voltage characteristics of Al₂O₃/AlGa_N/GaN structures and state density distribution at Al₂O₃/AlGa_N interface," Jpn. J. of Appl. Physic, vol. 50, n°2 (2011) 021001:1-7, <https://doi.org/10.1143/JJAP.50.021001>
- [6] M. A. Negara, D. Veksler, J. Huang, G. Ghibaudo, P. K. Hurley, G. Bersuker, N. Goel, and P. Kirsch, "Analysis of effective mobility and hall effect mobility in high-k based In_{0.75}Ga_{0.25}As metal-oxide-semiconductor high-electron-mobility transistors," Appl. Phys. Lett., vol. 99, no. 23 (2011), 232101:1-3, <https://doi.org/10.1063/1.3665033>.
- [7] Kevin J. Chen, L. Yuan, M. J. Wang, H. Chen, S. Huang, Q. Zhou, C. Zhou, B. K. Li, and J. N. Wang, "Physics of fluorine plasma ion implantation for GaN normally-off HEMT technology", Electron Devices Meeting (2011) 19:1-4, <https://doi.org/10.1109/IEDM.2011.6131585>.
- [8] L. Yuan, M. J. Wang, and K. J. Chen, "Fluorine plasma ion implantation in AlGa_N/GaN heterostructures: A molecular dynamics simulation study", Appl. Phys. Lett. 92(2008) 102109:1-3; <https://doi.org/10.1063/1.2896646>
- [9] G. Ghibaudo, "Transport in the inversion layer of a MOS transistor: use of Kubo-Greenwood formalism", J. Phys. C Solid State Phys., vol. 19, no. 5 (1986) 767–780, <https://doi.org/10.1088/0022-3719/19/5/015>
- [10] S. B. Lisesivdin, S. Acar, M. Kasap, S. Ozcelik, S. Gokden, and E. Ozbay, "Scattering analysis of 2DEG carrier extracted by QMSA in undoped $Al_{0.25}Ga_{0.75}N/GaN$ heterostructures", Semicond. Sci. Technol. 22 (2007) 543–548, <https://doi.org/10.1088/0268-1242/22/5/015>